Magneto-optical readout of dark exciton distribution in cuprous oxide

D. Fishman,[1] C. Faugeras,[2] M. Potemski,[2] A. Revcolevschi,[3] and P. H. M. van Loosdrecht[1,*]
[1]*Zernike Institute for Advanced Materials, University of Groningen, 9747 AG Groningen, The Netherlands*
[2]*Grenoble High Magnetic Field Laboratory, Centre National de la Recherche Scientifique, 25 Av. des Martyrs, 38 042 Grenoble, France*
[3]*Institut de Chimie Moléculaire et des Materiaux d'Orsay, Université de Paris Sud, UMR 8182, Bâtiment 410, 91405 Orsay Cedex, France*

(Received 28 February 2009; revised manuscript received 20 April 2009; published 21 July 2009)

An experimental study of the yellow exciton series in Cu_2O in strong magnetic fields up to 32 T shows the optical activation of direct and phonon-assisted paraexciton luminescence due to mixing with the quadruple allowed orthoexciton state. The observed phonon-assisted luminescence yields information on the statistical distribution of occupied states. Additional time-resolved experiments provide a unique opportunity to directly determine the time evolution of the thermodynamical properties of the paraexciton gas. Because the lifetime of paraexciton is hardly affected by the optical activation in a strong magnetic field, this opens new possibilities for studies aiming at Bose-Einstein condensation of excitons in bulk semiconductors.

DOI: 10.1103/PhysRevB.80.045208 PACS number(s): 71.35.Ji, 71.35.Lk, 78.20.Ls

I. INTRODUCTION

There is a number of well-established phenomena which evidence that composite bosons made of an even number of fermions, such as, for example, He-4 atoms, Cooper pairs, or alkali-metal atoms, behave under some conditions like ideal bosons which can condense into a macroscopic quantum state known as the Bose-Einstein condensate (BEC). One of the simplest forms of such a boson is the exciton, i.e., a bound electron-hole pair which characteristically appears as sharp emission and absorption features in the optical spectra of semiconductors and insulators. Strong indications exist that Bose-Einstein condensation of excitons, predicted a long time ago,[1] indeed occurs in man-made systems containing bilayer two-dimensional electron gases.[2] The excitons in these systems are formed under equilibrium conditions. The appearance of Bose-Einstein condensation of optically created, finite lifetime excitons is less evident.[3,4] Only complex systems such as, for example, excitonic polaritons in semiconductor microcavities provide signatures of a condensate phase.[5] The simplest system which has dominated the search for BEC in optically pumped solids is the excitonic gas in cuprous oxide, Cu_2O.[6] Since excitons in Cu_2O are strongly bound, their bosonic character persists up to high densities and temperatures and, due to the light masses of particles, their condensate form is expected at appealingly high temperatures. Cuprous oxide exhibits a number of exciton series, the lowest of which is the so-called yellow series just below the fundamental band gap, which by itself is again subdivided into the orthoexciton ($J=1$) and paraexciton ($J=0$) series.[6] Till recently, research has mainly focused on the triply degenerate optically active orthoexciton gas in cuprous oxide. It appears, however, that the lifetime of the orthoexciton, which is intrinsically limited by down conversion to the lower lying paraexciton state,[7] is too short to reach the condensed state.[8–11] In addition it has been proposed that the so-called "quantum saturation effect" prevents Bose-Einstein condensation of the orthoexciton gas in cuprous oxide.[8,9,12,13] In contrast, the lifetime for the paraexciton state, which is not optically active, is expected to be long. The exact value for the paraexciton lifetime varies widely from nanoseconds to milliseconds,[11,14–18] depending strongly on the quality of the sample, i.e., on the efficiency of nonradiative processes determined by the impurity and defect concentration. A significant population of the paraexciton state can be achieved via laser pumping of higher-energy, optically active states and the subsequent efficient relaxation processes toward the lowest singlet state. Advantageous on one side, the optical darkness of excitons at singlet state does not, however, allow to easily probe their properties and this has been one of the main obstacles in searching of their possible condensate form.

Although the direct optical absorption and emission to and from the paraexciton ground state are strictly forbidden, paraexcitons can radiatively decay with the assistance of Γ_5^- phonon.[3,19] In this process the spin flip is allowed by spin-orbit-lattice interaction. Unfortunately, the radiation efficiency is several orders of magnitude smaller than that of the orthoexcitons, requiring long integration time to detect the emission. Therefore one has to rely on the alternative methods to study the properties of the paraexcitons. One of the methods pursued so far has been to study the optically allowed interexciton transitions (similar to the Lyman series in the hydrogen spectrum).[16–18,20–22] Although one can easily extract basic parameters such as the effective mass and the lifetime of paraexcitons, it is more difficult to gain information on the statistical properties of the exciton gas from this kind of experiments. A second method is to break the symmetry, thereby optically activating direct and phonon-assisted transitions to and from the paraexcitonic ground state. There are many ways to break this symmetry, for instance, by applying pressure[23–25] and applying electric fields.[26] Though in particular the stress technique is quite promising, this perturbation typically leads to a considerable reduction in the lifetime of the paraexciton.[27] Application of a magnetic field breaks the symmetry in a more subtle way. In this case, the optically forbidden paraexciton state mixes with the quadruple-allowed orthoexciton state, leading to a weak paraexciton emission, which intensity is quadratic in the field, and a negligible influence on the lifetime. Early

studies already reported on the paraexciton magnetoluminescence,[28,29] although due to the relatively low magnetic fields, and the chosen crystal orientation these experiments did not allow for a detailed field-dependent study nor for a study of the statistical properties of the paraexciton gas. More recently, the optically forbidden paraexcitons were observed in fields up to 10 T. This work used resonant excitation to create an initially cold paraexciton gas and found a surprisingly narrow paraexciton magnetoabsorption line.[30,31]

In this paper we show that the application of sufficiently high magnetic fields is a noninvasive and subtle tool to activate both the direct and phonon-assisted emissions of the initially dark paraexcitons in Cu_2O. The observation of phonon-assisted emission provides a direct tool to probe the thermodynamical properties of paraexcitons gas in Cu_2O, and eventually, the appearance of its possible condensate phase.

II. EXPERIMENTAL DETAILS

In the present work, the paraexciton magnetoluminescence has been studied in a Faraday geometry with magnetic fields up to $B=32$ T at a temperature of $T=2$ K. This geometry was chosen to optimize both the degree of polarization as well as the emission efficiency.[29,32,33] For the steady-state experiments, platelets (thickness 200 μm) cut and polished from floating zone grown Cu_2O single crystals[34] of [110] orientation (denoted below as sample I) were placed in a pumped liquid-helium bath cryostat (1.3 K) and excited with the 532 nm line of a 100 mW solid-state laser. The circular polarized magnetoluminescence spectra[35] were detected using monochromator (resolution 0.02 nm) equipped with a LN_2-cooled charge coupled device (CCD) camera. Since the paraexciton lifetime of sample I was found to be less than 30 ns, indicating the presence of impurities, we used a [110] oriented 250-μm-thick platelet cut and polished from a high-purity Cu_2O natural crystal (denoted below as sample II) for the time-resolved experiments. A pulsed solid-state laser (50 ns, 4 kHz repetition rate, 523 nm, 0.6 mJ/cm^2) was used as an excitation source. The emitted light was detected with a single monochromator (resolution 0.06 nm) equipped with a fast CCD detector, yielding the time resolution of 30 ns.

III. RESULTS AND DISCUSSIONS

Figure 1 shows some typical luminescence spectra obtained for $B=0$ T [(a), unpolarized] and $B=32$ T [(b) right and (c) left, circularly polarized]. As expected, the $B=0$ T luminescence spectrum exhibits only orthoexcitonic features. Apart from the quadrupole allowed direct orthoexciton transition (O_0 at 2.034 eV), there are clear lines from phonon-assisted transitions involving Γ_5^- (O_1 at 11 meV), Γ_3^- (O_2 at 13.8 meV), and Γ_4^- (O_3 at 18.5 meV) phonons.[36] The presence of a magnetic field leads to two important changes in the spectra. First, the threefold degeneracy of the triplet orthoexciton state is lifted leading to a splitting of the orthoexciton derived bands (labeled $O_i^{m_J}$ in Fig. 1). The σ^+ and σ^- spectra show predominantly the $m_J=1$ and $m_J=-1$ components, respectively. Second, and more interestingly for the present work, a number of emission features appear in the spectra, which are not polarized. The sharp feature at 2.0216 eV originates from direct emission from the paraexciton $1s$ to the ground state (P_0). In addition, like for the orthoexciton, two phonon-assisted paraexciton recombination lines are observed at 2.011 eV (P_1, Γ_5^- phonon) and 2.008 eV (P_2, Γ_3^-). The emission line observed at 2.004 eV cannot unambiguously be assigned to the Γ_4^- phonon-assisted paraexciton transition, since this transition is expected at 2.0035 eV. However, both the lineshape as well as the field dependence of the intensity and paramagnetic shift of this line are in very good agreement with the paraexciton phonon-assisted lines.

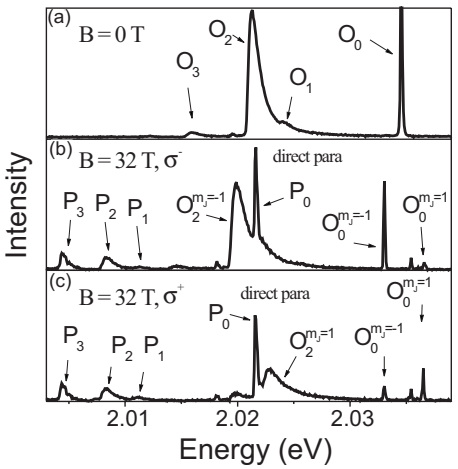

FIG. 1. Exciton magnetoluminescence spectra of sample I at bath temperature $T=2$ K. (a) Unpolarized luminescence at $B=0$ T. O_0: direct orthoexciton emission; O_1-O_3: phonon-assisted orthoexciton emission involving Γ_5^- (11 meV), Γ_3^- (13.8 meV), and Γ_4^- (18.5 meV) phonons, respectively. (b) and (c) Circularly polarized [(b) σ^+ and (c) σ^-] luminescence at $B=32$ T. P_0: direct paraexciton emission; P_1 and P_2: phonon-assisted paraexciton emission involving Γ_5^- and Γ_3^-, respectively.

As is the case for orthoexcitons, the phonon-assisted emission lines may provide information on the statistical properties of the optically excited paraexciton gas. Before turning to these properties, we first discuss some of the more general features of the paraexciton and orthoexciton emissions. The reason that the paraexciton lines are activated in a magnetic field is the presence of the perturbing Zeeman term in the electron-hole Hamiltonian

$$V = \frac{1}{2}\mu_B(g_e S_e^z B_z + g_h S_h^z B_z), \tag{1}$$

leading to a mixing of the singlet paraexciton state $|S\rangle$ with the $m_J=0$ triplet orthoexciton state $|T_0\rangle$. The perturbed singlet state becomes

$$|S\rangle_B = |S\rangle_0 - \frac{(g_e - g_h)\mu_B B}{\Delta + \sqrt{\Delta^2 + (g_e - g_h)^2 \mu_B^2 B^2}}|T_0\rangle_0, \tag{2}$$

where $g_e(g_h)$ is the electron (hole) g factor, μ_B the Bohr magneton, and $\Delta=12$ meV the energy difference between the orthoexciton and paraexciton ground states. This mixing

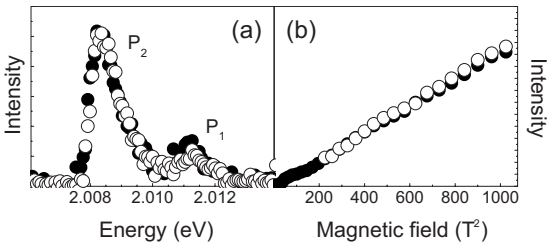

FIG. 2. (a) Right (open circles) and left (filled circles) circularly polarized phonon-assisted paraexciton emission at $T=2$ K, $B=32$ T (sample I). P_1 and P_2 refer to Γ_5^- and Γ_3^- phonon-assisted transitions, respectively. (b) Intensity of the Γ_3^--phonon-assisted paraexciton emission (closed circles) and direct paraexciton emission (open circles) as a function of the squared magnetic field.

leads to a nonzero paraexciton luminescence intensity, which in the limit $(g_e-g_h)\mu_B B \ll \Delta$, as is the case in the experiments, will be proportional to the square of the magnetic field. Moreover, since the mixing occurs with the $m_J=0$ state only, one expects a linear polarization for the paraexciton emission. Experimentally, these features are indeed observed, as is shown in Figs. 2(a) and 2(b): there is no difference in paraexciton emission intensity for σ^+ and σ^- polarized spectra [Fig. 2(a)], and the intensity is indeed quadratic in fields up to 32 T [Fig. 2(b)]

A second consequence of the mixing is that the energies of the states involved show a diamagnetic shift. The field-dependent energy of the paraexciton state is given by

$$E_S(B) = E_S(0) + \frac{1}{2}[\Delta - \sqrt{\Delta^2 + (g_e - g_h)^2 \mu_B^2 B^2}]. \qquad (3)$$

In the same low-field limit as before, this reduces to $E_S(B) \approx E_S(0) - (g_e-g_h)^2 \mu_B^2 B^2/4\Delta$. Similarly, the energy of the $m_J=0$ orthoexciton state is expected to shift to higher energy by the same amount.

These diamagnetic shifts are nicely demonstrated in Fig. 3, which shows a two-dimensional false color map of the orthoexciton and paraexciton emission intensities as a function of energy and field. In the presence of a magnetic field, the single Γ_5^+ orthoemission line observed at $B=0$ T splits into its $m_J=-1,0,1$ components [Fig. 3(a)]. The same holds for the phonon-assisted orthoexciton lines [Fig. 3(b)]. While the $m_J=1$ (σ^+) and $m_J=-1$ (σ^-) lines show their expected linear Zeeman splitting, the energy of $m_J=0$ line indeed increases quadratically with increasing field. In line with this, the paraexciton line shows, once observable, a quadratically deceasing energy on increasing field [Fig. 3(b)]. However, even though Eq. (3) predicts equal size shifts for the ortho and paraexcitons, the shift for the orthoexciton at $B=32$ T (0.31 meV) is about half of the value observed for the paraexciton (0.57 meV), see Fig. 3(c). The origin of this discrepancy is presently not clear, although it has been suggested that it is due to the interaction of the orthoexciton with higher lying levels.[37]

In principle one can extract the values of the electron and hole g factors from the observed energy shifts.[38] Assuming that the paraexciton indeed shifts according to Eq. (3) leads to the relation $(g_e-g_h)^2=7.5$. An independent relation can be

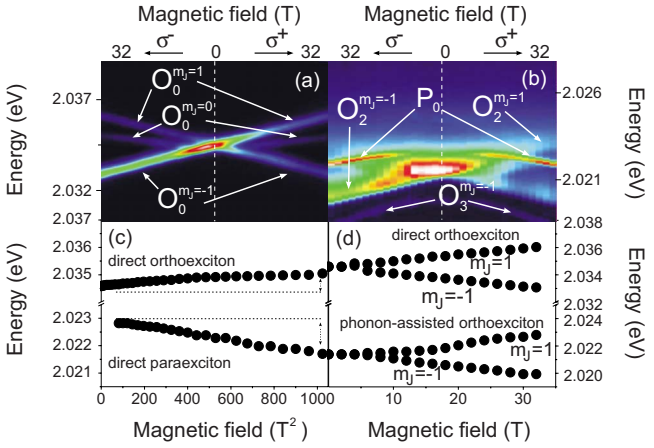

FIG. 3. (Color online) Two-dimensional image of the field dependence of the $1s$ orthoexciton spectra for sample I at $T=2$ K in the energy range of (a) the direct emission and (b) the phonon-assisted emission. (c) Energy of the direct paraexciton and $m_J=0$ orthoexciton emission as a function of the magnetic field squared at $T=2$ K. (d) Energy position of orthoexciton lines as a function of the magnetic field at $T=2$ K.

obtained from the observed Zeeman splitting, shown in more detail in Fig. 2(d), yielding $|g_e+g_h|=1.66$. These values are in good agreement with previously reported values,[29,37–39] and lead to either $g_e=2.68$, $g_h=-1.02$ or the reverse.

Finally, we return to the phonon-assisted paraexciton lines and the statistical properties of the paraexciton gas. Figure 4 (symbols) shows the experimental Γ_3^- and Γ_5^- phonon-assisted lines at $T=2$ K for $B=32$ T. Assuming energy-independent exciton-phonon coupling matrix elements and dispersionless phonons with energy $\hbar\Omega$, the emission at a certain energy is given by[3,9]

$$I(E) \propto \sum_i D(E - E_0 - \hbar\Omega_i) f(E - E_0 - \hbar\Omega_i), \qquad (4)$$

where i labels the phonons, E_0 is the energy of the $\mathbf{k}=0$ paraexciton, $D(E) \propto \sqrt{E}$ is the density of excitonic states, and

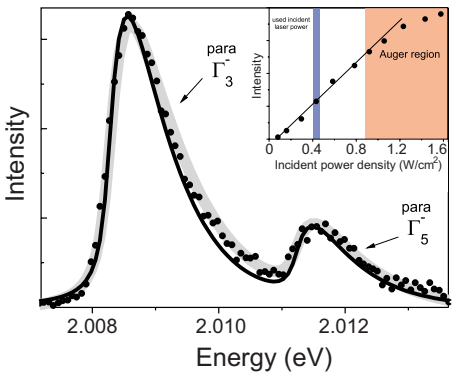

FIG. 4. (Color online) Phonon-assisted paraexciton emission at $T=2$ K, $B=23$ T. Open circles—experimental data; black line—theoretical model using Maxwell-Boltzmann distribution ($T=7.3$ K); and gray line—theoretical model using Bose-Einstein distribution ($T=8$ K, $\mu=-0.5$ meV). Inset: the integrated intensity of phonon-assisted luminescence as a function of the excitation power density.

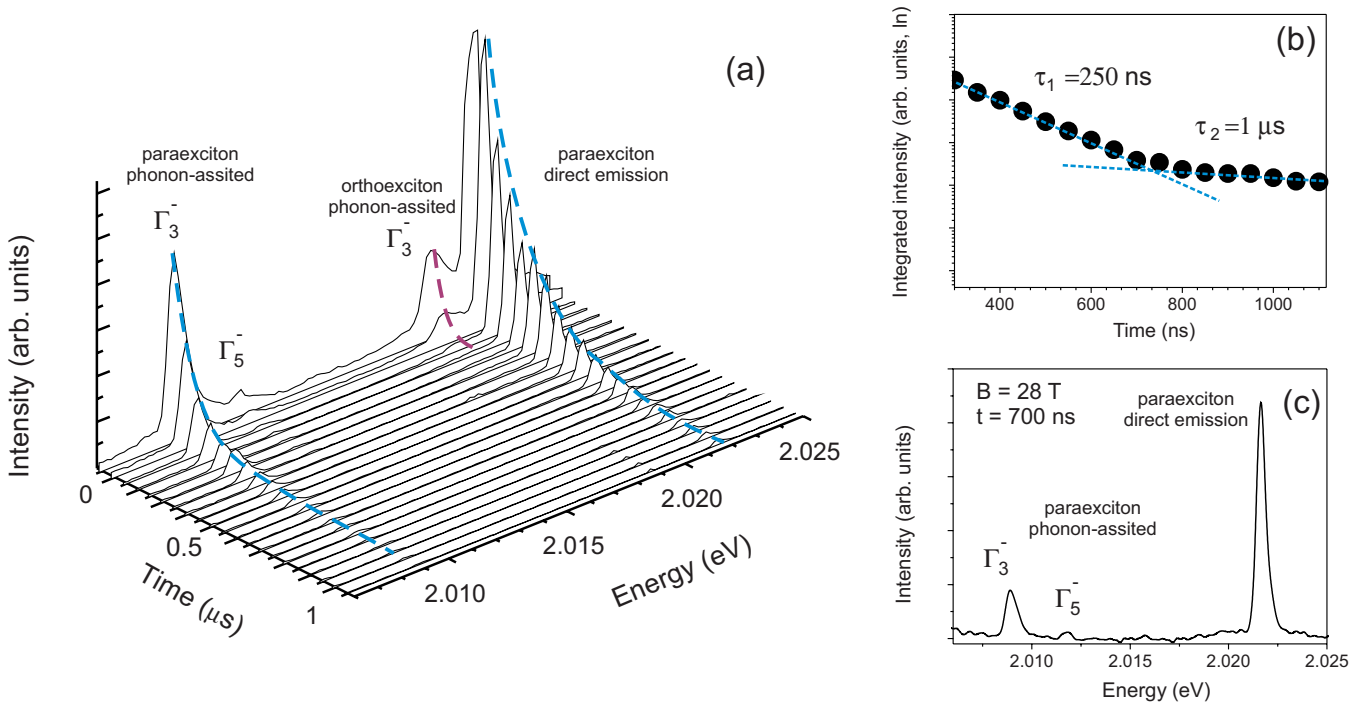

FIG. 5. (Color online) (a) Exciton luminescence at different times after the excitation with 50 ns pulse of 523 nm wavelength at $T=2$ K, $B=28$ T for sample II (pump energy density of 0.6 mJ/cm^2). (b) The magnetoluminescence spectrum of the paraexciton gas at 600 ns after the excitation for sample II.

$f(E)$ is the statistical distribution function for the excitons.

The experimental spectrum is given by convolution of Eq. (4) with the known experimental resolution (0.1 meV). The drawn black line in Fig. 4 represents a fit of the convoluted Eq. (4) to the data using the classical Maxwell-Boltzmann distribution, appropriate for the current experiments. The parameter extracted from the fit is an exciton gas temperature $T_{\mathrm{MB}}=7.3$ K. An important parameter one would like to extract from the experiment is the density of excited paraexcitons. A straightforward, though inaccurate, method is to assume that each absorbed photon creates exactly one exciton, which is then allowed to diffuse throughout the sample volume. Taking a penetration depth of 30 μm,[9] the current experimental conditions lead to an estimated density of $\sim 10^{16}$ cm^{-3}. This value may be taken as an upper limit since the estimate does not take diffusion into account which will lead to a substantially smaller density in the actual experiment. For demonstration purposes, one could analyze the luminescence line shape using the Bose-Einstein distribution, i.e., assuming quantum statistics, and from the extracted gas temperature and chemical potential calculate the density. The legitimacy of this analysis, in particular, the use of Bose-Einstein distribution function, has, however, been questioned in Ref. 40. It is suggested, that Auger processes might lead to an overestimation of the exciton density and that the competition between Auger recombination and cooling of the phonon emission could possibly result in a Bose-type "distribution." To avoid this problem, the current experiments have been performed at moderate excitation densities, where Auger processes are playing only a minor role. This is illustrated in the inset of Fig. 4, which shows the excitation power dependence of the intensity of the phonon-assisted paraexciton emission at $B=23$ T. For low powers the emission scales linearly with the excitation power. The influence of Auger processes is observed only for excitation power densities exceeding 0.8 W/cm^2, where the intensity shows the typical sublinear behavior with increasing power. Similar results were observed in Refs. 41 and 42 for the orthoexciton luminescence: the intensity increases by the square root of the excitation density. In present experiments, the used incident power had a value well below "Auger regime" (0.4 W/cm^2) ensuring that Auger process play a minor role only.

A convolution of Eq. (4) using quantum statistics has also been fitted to the data presented in Fig. 4 (gray curve). The parameter extracted from the fit is an exciton gas temperature $T_{\mathrm{BE}}=8$ K and a chemical potential $\mu=-0.5$ meV. For the exciton gas to be truly in the quantum limit, the density has to be higher than or at least comparable to the quantum density $n_Q=(\frac{mk_BT}{2\pi\hbar^2})^{3/2}$. For a paraexciton gas at 8 K this means a density of $\sim 2\times 10^{18}$ cm^{-3}. Using the obtained chemical potential and temperature extracted from the fit, the calculated density of the exciton gas gives an upper estimate of 10^{15} cm^{-3}, i.e., much smaller than the quantum density. Despite the apparently good fit, this internal inconsistency demonstrates that indeed the exciton gas is still in the classical limit, and one has to go to much lower temperature or higher densities to reach the quantum limit.

In addition to the above-described continuous-wave experiments, we have also performed time-resolved experiments to elucidate the dynamics of the paraexciton gas. Sample II was used for these experiments since it shows a relatively long paraexciton lifetime. Figure 5(a) shows some typical time-resolved magnetoluminescence spectra at

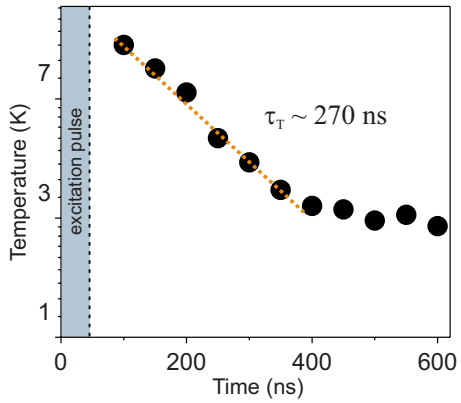

FIG. 6. (Color online) Time evolution of the paraexciton gas temperature T_{MB}. Excitation with 50 ns pulse of 523 nm wavelength. Bath temperature $T=2$ K, sample II.

$T=2$ K, $B=28$ T. At early times, the spectrum shows the clear presence of both orthoexcitons and paraexcitons. As expected, the orthoexcitonic features vanish rapidly due to ortho-to-paraexciton conversion. In contrast, the paraexcitons have a fairly long lifetime even at these high fields. The observed decay is clearly not monoexponential, as demonstrated in Fig. 5(b). It reveals a fairly complicated behavior. There is a fast initial decay which closely follows the pump-pulse profile (60 ns). Directly after the pump pulse, a fast decay occurs with a time constant of ~250 ns leading to a reduction in the density by about two orders of magnitude within the first 600 ns. This decay is most likely due to the collision-induced nonradiative decay process.[16] This is in line with the high-power density used in this experiment. A simple estimate yields an upper limit for the initial density of about 10^{17} cm^{-3}, which is well within the Auger regime. Finally after 600 ns Auger processes do not play an essential role anymore (the density dropped below 10^{15} cm^{-3}), and the luminescence intensity slowly decays further with a time constant of around 1 μs, mainly limited by the purity of the sample.

Using the method described above, one can again extract an estimate of the gas temperature (using a classical Maxwell-Boltzmann distribution function) as a function of time after excitation. The evolution of the estimated paraexciton gas temperature presented in Fig. 6 shows that there is a fast initial cooling with a time constant of 270 ns. This decay time is comparable to that observed for the intensity decay, suggesting that also for the cooling, Auger processes play a dominant role. After about 500 ns the gas has cooled down to about 2 K. This temperature corresponds to the bath temperature, i.e., the gas has reached thermodynamical equilibrium at these times.

IV. CONCLUSION

In conclusion, we have studied the magneto-optical properties of the yellow exciton series in cuprous oxide in magnetic fields up to 32 T. We observed the direct emission of the normally optically inactive paraexciton arising from mixing of the 1s paraexciton state with the 1s $m_J=0$ orthoexciton state. The experimental results can be well explained using first-order perturbation theory. Due to the gentle breaking of the symmetry by the magnetic field, the lifetime of excitons is only weakly affected allowing efficient thermalization of the exciton gas. Besides the direct emission of the paraexciton, we also observe additional lines, which are assigned to phonon-assisted emission processes from the paraexciton state, involving various phonons of different symmetries, similar to the orthoexciton case. These lines provide a unique opportunity for direct determination of the thermodynamical properties of the paraexciton gas. From the present experiments, the density of the exciton gas is well below the quantum density. The time evolution of the gas parameters, obtained from time-resolved experiments is calling for further experimental efforts at higher exciton densities and possible lower temperatures to solve the enigma of BEC in Cu_2O.

ACKNOWLEDGMENTS

We thank Foppe de Haan (University of Groningen) for assistance in data treatment. We also would like to thank Makoto Kuwata-Gonokami (University of Tokyo) for helpful discussions and for providing the high-purity natural sample (sample II). This work was partially supported by the European Access Program under Contact No. RITA-CT-2003-505474 and the Grenoble High Magnetic Fields Laboratory (CNRS, France).

*p.h.m.van.loosdrecht@rug.nl

[1] L. V. Keldysh and A. N. Kozlov, Sov. Phys. Solid State **6**, 2219 (1965).
[2] J. P. Eisenstein and A. H. MacDonald, Nature (London) **432**, 691 (2004).
[3] D. W. Snoke, J. P. Wolfe, and A. Mysyrowicz, Phys. Rev. Lett. **64**, 2543 (1990).
[4] L. V. Butov, Solid State Commun. **127**, 89 (2003).
[5] J. Kasprzak, M. Richard, S. Kundermann, A. Baas, P. Jeambrun, J. M. J. Keeling, F. M. Marchetti, M. H. Szymanska, R. Andre, J. L. Staehli, V. Savona, P. B. Littlewood, B. Deveaud, and Le Si Dang, Nature (London) **443**, 409 (2006).
[6] A. Griffin, D. W. Snoke, and S. Stringari, *Bose-Einstein Condensation* (Cambridge University Press, Cambridge, 1995).
[7] D. W. Snoke, D. P. Trauernicht, and J. P. Wolfe, Phys. Rev. B **41**, 5266 (1990).
[8] D. Snoke, J. P. Wolfe, and A. Mysyrowicz, Phys. Rev. Lett. **59**, 827 (1987).
[9] K. Karpinska, M. Mostovoy, M. A. van der Vegte, A. Revcolevschi, and P. H. M. van Loosdrecht, Phys. Rev. B **72**, 155201 (2005).
[10] *Bose-Einstein Condensation of Excitons and Biexcitons and Coherent Nonlinear Optics with Excitons*, edited by S. A. Moskalenko and D. W. Snoke (Cambridge University Press, Cam-

bridge, UK, 2005).
[11] S. Denev and D. W. Snoke, Phys. Rev. B **65**, 085211 (2002).
[12] Y. C. Lee and W. Zhu, J. Phys.: Condens. Matter **12**, L49 (2000).
[13] G. M. Kavoulakis, Phys. Rev. B **65**, 035204 (2001).
[14] A. Mysyrowicz, D. Hulin, and A. Antonetti, Phys. Rev. Lett. **43**, 1123 (1979).
[15] J. I. Jang, K. E. O'Hara, and J. P. Wolfe, Phys. Rev. B **70**, 195205 (2004).
[16] K. Yoshioka, T. Ideguchi, and M. Kuwata-Gonokami, Phys. Rev. B **76**, 033204 (2007).
[17] D. A. Fishman, A. Revcolevschi, and P. H. M. van Loosdrecht, Phys. Status Solidi C **3**, 2469 (2006).
[18] K. Karpinska, P. H. M. van Loosdrecht, I. P. Handayani, and A. Revcolevschi, J. Lumin. **112**, 17 (2005).
[19] K. E. O'Hara, L. Ó Súilleabháin, and J. P. Wolfe, Phys. Rev. B **60**, 10565 (1999).
[20] A. Jolk, M. Jorger, and C. Klingshirn, Phys. Rev. B **65**, 245209 (2002).
[21] M. Kuwata-Gonokami, M. Kubouchi, R. Shimano, and A. Mysyrowicz, J. Phys. Soc. Jpn. **73**, 1065 (2004).
[22] M. Kubouchi, K. Yoshioka, R. Shimano, A. Mysyrowicz, and M. Kuwata-Gonokami, Phys. Rev. Lett. **94**, 016403 (2005).
[23] J. L. Lin and J. P. Wolfe, Phys. Rev. Lett. **71**, 1222 (1993).
[24] N. Naka and N. Nagasawa, Phys. Status Solidi B **238**, 397 (2003).
[25] N. Naka and N. Nagasawa, Solid State Commun. **126**, 523 (2003).
[26] A. R. H. F. Ettema and J. Versluis, Phys. Rev. B **68**, 235101 (2003).
[27] N. Naka and N. Nagasawa, Phys. Rev. B **65**, 075209 (2002).
[28] S. V. Gastev, E. L. Ivchenko, G. E. Pikus, N. S. Sokolov, and N. L. Yakovlev, Fiz. Tverd. Tela (Leningrad) **25**, 3002 (1983).
[29] S. Kono and N. Nagasawa, Solid State Commun. **110**, 93 (1999).
[30] J. Brandt, D. Fröhlich, C. Sandfort, M. Bayer, H. Stolz, and N. Naka, Phys. Rev. Lett. **99**, 217403 (2007).
[31] C. Sandfort, J. Brandt, D. Fröhlich, M. Bayer, and H. Stolz, Phys. Rev. B **78**, 045201 (2008).
[32] R. J. Elliott, Phys. Rev. **124**, 340 (1961).
[33] N. L. Yakovlev and N. S. Sokolov, Fiz. Tverd. Tela (Leningrad) **26**, 471 (1984).
[34] R. D. Schmidt-Whitley, M. Martinez-Clemente, and A. Revcolevschi, J. Cryst. Growth **23**, 113 (1974).
[35] Luminescence spectra are only 85% polarized due to the experimental conditions.
[36] *Polarons in Ionic Crystals and Polar Semiconductors*, Proceedings of the 1971 Antwerp Advanced Study Institute on Fröhlich Polarons and Electron-Phonon Interaction in Polar Semiconductors, edited by J. T. Devreese (North-Holland, Amsterdam, 1972).
[37] G. Kuwabara, M. Tanaka, and H. Fukutani, Solid State Commun. **21**, 599 (1977).
[38] M. Cartier, J. B. Grun, and S. Nikitine, J. Phys. (France) **25**, 361 (1966).
[39] D. Fröhlich and R. Kenklies, Phys. Status Solidi B **111**, 247 (1982).
[40] K. E. O'Hara and J. P. Wolfe, Phys. Rev. B **62**, 12909 (2000).
[41] D. P. Trauernicht, J. P. Wolfe, and A. Mysyrowicz, Phys. Rev. B **34**, 2561 (1986).
[42] J. I. Jang and J. P. Wolfe, Solid State Commun. **137**, 91 (2006).